Liquid and gas-liquid phase behavior in thermopneumatically actuated microvalves

Albert K. Henning[†]

Redwood Microsystems, Inc., 959 Hamilton Avenue, Menlo Park, CA 94025

ABSTRACT

Thermopneumatically actuated microvalves rely on the thermal expansion of a gas, liquid, or gas-liquid mixture, hermetically sealed within an actuation cavity. This cavity is, typically, mechanically rigid on all sides, except for the side containing a mechanically flexible membrane, which is responsible for controlling the flow of fluid in the microvalve. Taken as a system, this actuation technique requires simultaneous consideration of the mechanical behavior of the membrane, the mechanical behavior of the control fluid, and the coupled thermal behavior of the valve and control fluid.

Previous work has discussed the details of the liquid and gas-liquid behavior of the hermetically-sealed control fluid[1]. Figures of merit were developed for membrane behavior as a function of Young's modulus, valve structural parameters, and some of the thermodynamic properties of the thermopneumatic control fluid. However, the effects of initial thermodynamic state of the control fluid, external temperature (including thermal gradient), external pressure, and the temperature boundary condition at the control fluid's heat source were not considered. In this work, these effects are considered quantitatively. A model for the steady-state valve behavior (membrane deflection versus input heater power) is developed. The utility of this model in designing microvalves for gas and liquid flow control is also demonstrated.

Keywords: MEMS, microvalve, microfluidics, thermopneumatic actuation, gas-liquid phase transition

LIST OF VARIABLES

T_f	temperature (K) at which the thermopneumatic cavity is filled
T_a	ambient temperature (K)
T_{sat}	saturation temperature (K) [defines the gas-liquid physical boundary]
T_r	heater resistor temperature (K)
$A,B,C,D,C"$	constants related to thermopneumatic fluid thermodynamic properties
a	membrane radius (m)
h	membrane thickness (m)
z_0	vertical thickness of the cavity at the fill temperature (m)
V_0	volume of the cavity at the fill temperature (m)
dV	total cavity volume change (m)
dV_l, $\boldsymbol{d}_l$	cavity volume change due to expansion of the thermopneumatic liquid (m)
$\boldsymbol{d}_g$	cavity volume change due to expansion of the thermopneumatic gas (m)
Δz	total membrane displacement due to expansion of the thermopneumatic liquid and gas (m)
$\boldsymbol{r}_l$	thermal resistivity of the thermopneumatic liquid (W/m-K)$^{-1}$
$\boldsymbol{r}_g$	thermal resistivity of the thermopneumatic gas (W/m-K)$^{-1}$
$\boldsymbol{b}$	coefficient of thermopneumatic liquid thermal expansion (1/K)
R	universal gas constant (8314 m^2/sec^2-K, divided by gas molecular weight)
P_l	pressure in the cavity due to thermopneumatic liquid (Pa)
P_g	pressure in the cavity due to thermopneumatic gas (Pa)
P	pressure in the cavity (Pa)
P_a	ambient pressure (Pa)
E, μ	Young's modulus (1.9 x 10^{11} Pa), Poisson ratio (0.09) for silicon

[†] Email: henning@redwoodmicro.com; WWW: http://www.redwoodmicro.com; Telephone: 650-617-0854; FAX: 650-326-9217

1. INTRODUCTION

Scientific and technological interests in microfluidics have increased during the past decade. Microvalves have drawn particular attention in efforts to control and distribute flow on the microscale.[2] Such devices can be actuated using bimetallic,[3] shape-memory alloy,[4] electrostatic,[5] pneumatic,[6] electrochemical,[7] or thermopneumatic[8] means. Applications range from mass-flow controllers for semiconductor manufacture,[9] to refrigerant liquid control systems,[10] to biomedical applications (such as gas or liquid chromatography),[11] and to devices to control flow over airfoil surfaces.[12]

The relative merits of each actuation means have been compared.[1] Thermopneumatic actuation provides the greatest mechanical work per unit volume, as well as exceptional flow resolution.[9] However, since thermal energy is employed to extract the available mechanical work, thermopneumatic valves tend to be slower than some of their counterparts. It is desirable to maintain a liquid-only phase in a sealed thermopneumatic actuation cavity, though the phase transition between liquid and gas may offer a means to achieve higher actuation speeds.

From a theoretical perspective, virtually no work has been done in the area of liquid-gas phase transitions in sealed cavities at the microscale. The addition of a deformable mechanical boundary for one wall of the cavity complicates the system, as does the addition of a non-uniform temperature distribution, and external pressure variations. Some relevant work in this area may be found in the phase transition of binary mixtures.[13]

This work develops a general, one-dimensional model for the relationship between the position of a microvalve membrane diaphragm, and the temperature boundary condition in the microvalve. Secondary variables explored are ambient pressure, ambient temperature, and the initial thermodynamic state variables of the thermopneumatic fluid. The results are applied to a simple microvalve design problem.

2. DEFINITIONS

Figure 1 provides a schematic cross-section of a thermopneumatically-actuate microvalve, for use as reference in the development of this model. The microvalve consists of three layers: a flow distribution (or valve seat) layer; a membrane or diaphragm layer, for providing closure against the valve seat; and a layer to provide the hermetic seal of the thermopneumatic cavity. Typical dimensions and materials are: 1 mm for the seal layer, comprised of Pyrex; 0.5 mm for each of the membrane and valve seat layers, comprised of silicon; membrane thickness of 0.05 mm; thermopneumatic cavity depth of 0.1-0.3 mm; lateral membrane dimensions of 4 mm; overall lateral valve size of 6 mm.
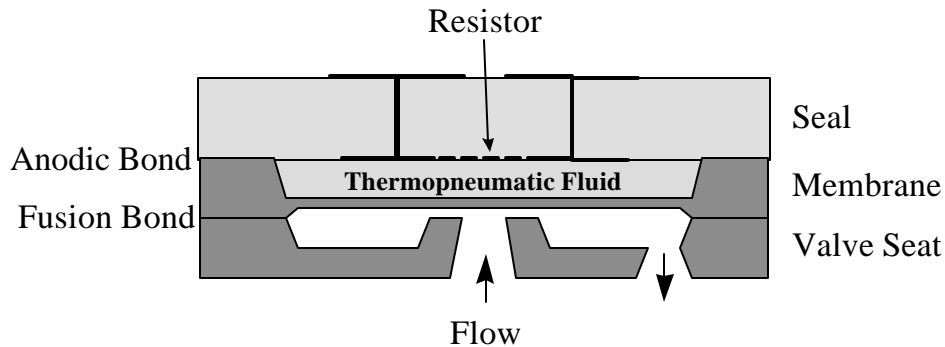

Figure 1: *Cross-section of a thermopneumatically-actuated, normally-open, proportional flow microvalve.*

Figure 2 shows how the different layers are defined mechanically for the one-dimensional model. The top edge represents the (mechanically fixed) boundary of the thermopneumatic cavity layer, while the bottom edge represents the (mechanically movable) boundary of the membrane. A fill procedure is used to introduce the thermopneumatic fluid to the cavity, prior to sealing.

Figure 3 defines the one-dimensional thermal model (or, temperature boundary conditions) employed. The hermetic seal layer is taken to have a resistor applied to it, which provides the thermal boundary condition related to the input power. The

saturation temperature between a gas-liquid boundary, and the ambient temperature, are also shown. The temperature at which the cavity is filled may not be the same as either the ambient temperature, or the resistor temperature, during valve operation.

Figure 4 shows the pressure-enthalpy diagram which explains the thermal model in a thermodynamic context (relative to the gas-liquid state of the thermopneumatic fluid inside cavity). This diagram allows an analytical relationship to be determined, between the pressure in the hermetically sealed cavity, and the saturation temperature, as described in the next section.
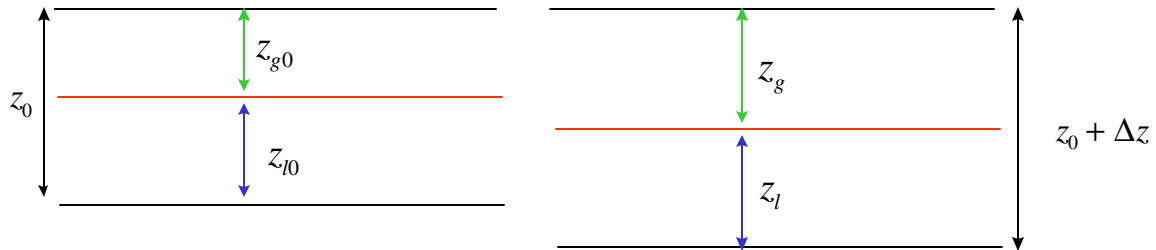

Figure 2: Definition of layers. Left: Initial state, at fill temperature and pressure. Right: State for given ambient pressure, ambient temperature, resistor temperature.
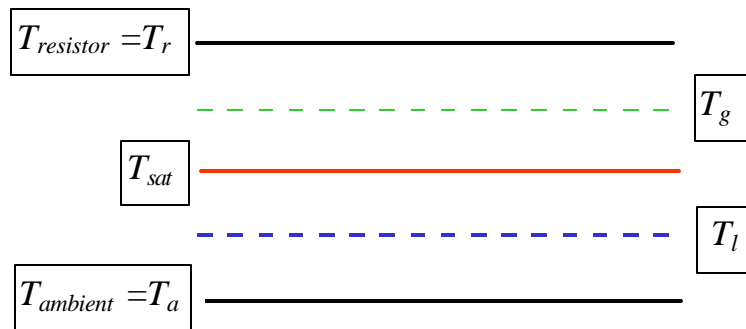

Figure 3: Definition of temperature boundary conditions. T_{sat} defines the boundary between the liquid and gas layers.
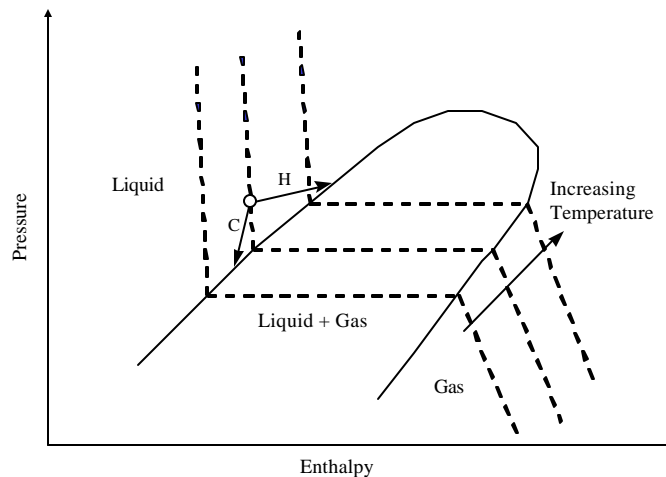

Figure 4: Thermodynamic P-h diagram for the model. Dashed lines indicate isotherms. The typical, initial fill state is shown as a white circle. As the system cools, the thermopneumatic fluid follows the path "C". Once the vapor dome is crossed, two phases exist (cavitation), and the pressure in the cavity is set by the saturation temperature located (spatially) between the gas and liquid phases. As the system heats, the fluid follows the path "H". When the vapor dome is crossed, two phases exist (evaporation, or boiling), and again the pressure is set by the saturation temperature at the spatial location between the two phases. Prior to crossing the vapor dome, the pressure is set solely by the incompressible liquid.

3. ASSUMPTIONS

In order to develop a workable model, a number of assumptions must be made. These are:

- The hermetically-sealed cavity is isobaric.
- Linear thermal models are valid, so that $T_g=(T_r+T_{sat})/2$ and $T_l=(T_a+T_{sat})/2$.
- The gas is (typically) therefore super-heated, and the liquid is sub-cooled.
- The volume fraction of liquid during the fill procedure, $\boldsymbol{h}$ does not change as a function of temperature. That is, the mass of fluid converted to gas is taken to be negligible compared to the total fluid mass.
- The system is largely one dimensional, and the heat transfer is purely conductive.
- Due to the high thermal conductivity of silicon, the membrane temperature is equal to the ambient temperature.

4. THEORY

The procedure consists first of writing the system equations for the valve. These equations are a function of either the resistor temperature (if there is only liquid in the thermopneumatic fluid cavity), or the saturation temperature at the gas-liquid interface. Then, the equations are solved self-consistently for T_r or T_{sat}.

4.1 Thermal Behavior of the System

The system thermal behavior is described in Equation (1). It is derived from Figure 2, by applying steady-state, linear thermal heat transfer analysis. Physically, the saturation temperature lies between the resistor and ambient temperature boundary conditions. Note that, if the cavity is filled only with liquid, then $T_{sat}=T_r$. Also, note that, if $T_r=T_a$, a vapor can still exist in the cavity, depending upon the relationship between T_r and T_f.

$$\frac{T_r - T_{sat}}{\boldsymbol{r}_g z_g} = \frac{T_{sat} - T_a}{\boldsymbol{r}_l z_l} \tag{1a}$$

$$\Rightarrow z_g = z_l \frac{\boldsymbol{r}_l}{\boldsymbol{r}_g} \frac{T_r - T_{sat}}{T_{sat} - T_a} \tag{1b}$$

Several other functional relationships relate the gas and liquid volumes. These are:

$$z_g = z_{g0} + \boldsymbol{dz}_g = (1-\boldsymbol{h})z_0 + \boldsymbol{dz}_g \tag{2a}$$

$$z_l = z_{l0} + \boldsymbol{dz}_l = \boldsymbol{h}z_0 + \boldsymbol{dz}_l \tag{2b}$$

$$\Delta z = \boldsymbol{dz}_g + \boldsymbol{dz}_l \tag{2c}$$

Δz is the departure of the membrane from its equilibrium position, termed the 'stroke'. The factor $\boldsymbol{h}$ represents the fraction of the initial cavity volume which is liquid. [Note that, in the strict sense, this factor changes as a function of temperature and pressure. However, since the specific volume (volume per weight) is so much greater for the gas phase than the liquid phase, this additional complication is ignored.]

4.2 Thermomechanical (thermopneumatic) Behavior of the Thermopneumatic Liquid

If we take the membrane to be circular, then the change in volume associated with temperature changes in the thermopneumatic liquid has been determined from:

$$dV = \frac{1}{6}\boldsymbol{p} \cdot \Delta z \cdot (3a^2 + \Delta z^2) \cong \frac{1}{2} \cdot \boldsymbol{p} \cdot \Delta z \cdot a^2 \tag{3a}$$

$$dV_l = \boldsymbol{b}V_0(T_l - T_f) \tag{3b}$$

$$V_0 = \boldsymbol{p}a^2 z_0 \tag{3c}$$

$$\Delta z = 2\boldsymbol{b}z_0(T_l - T_f) = \boldsymbol{b}z_0(T_{sat} + T_a - 2T_f) \tag{3d}$$

These expressions presume no gas phase is present, which is appropriate when finding the pressure associated with an incompressible liquid. The first expression is the volume of a circular membrane which has been spherically displaced according to a stroke Δz. The second expression has utilized the factor $\boldsymbol{b}$ which is the coefficient of thermal expansion of the thermopneumatic liquid. The third expression is another geometrical relation between the volume and the cavity depth. The fourth expression is the combination of the first three, but only when $dV = dV_l$ (that is, when all the membrane deflection is due to the liquid).

This use of $\boldsymbol{b}$ assumes it is a constant of temperature. For the work below, analysis is done using the materials properties of Fluorinert™ electronic liquids. These liquids are weakly temperature dependent, based on Equation (4) and the information shown in Table I. The properties of other fluids are given elsewhere.[1] For the purposes of this study, $\boldsymbol{b}$ will be taken to be temperature dependent. The volumetric expansion of the Fluorinert™ liquid needs to be determined using:

$$\boldsymbol{d}z_l = \boldsymbol{h}z_0 \int_{T_f}^{T_l} \boldsymbol{b}(T)dT \tag{4a}$$

$$\boldsymbol{d}z_l = \boldsymbol{h}z_0 \ln\left(\frac{C''-T_f}{C''-T_l}\right) = \boldsymbol{h}z_0 \ln\left(\frac{C''-T_f}{C'' - \dfrac{T_{sat} + T_a}{2}}\right) \tag{4b}$$

Table I: Constants for Fluorinert™ Liquids

Constant	FC-72	FC-84	FC-77	FC-104	FC-75	FC-40	FC-43	FC-70	FC-71
A	7.6042	8.0166	8.0915	8.5860	8.2502	8.2594	8.3586	8.9087	9.0190
B	1562	1824	1928	2126	2018	2310	2453	2939	3229
C	1.740	1.790	1.838	1.819	1.825	1.903	1.913	1.984	2.002
D	.00261	.00257	.00245	.00248	.00246	.00215	.00218	.00193	.00224
C"=C/D+273	939.7	969.5	1023.2	1006.5	1014.9	1158.1	1150.5	1301.0	1166.8

4.3 Mechanical (Pneumatic) Behavior of the Membrane

Based on mechanical considerations, the stroke of the membrane is given by:

$$\Delta z = 0.0151 \cdot (1 - \boldsymbol{m}^2) \cdot a \cdot \left(\frac{a}{h}\right)^3 \cdot \frac{P - P_a}{E} \tag{5}$$

Equation (5) comes from the text by di Giovanni,[14] and is derived for single crystal silicon membrane deflections. The stroke of the membrane is related to the difference between the absolute pressure P in the cavity, and the ambient pressure. [Note that this formulation allows the prediction of negative membrane deflection, or stroke ($\boldsymbol{d} < 0$ for $P < P_a$).] For a gas-liquid phase inside the cavity, it is easiest to determine this pressure (in units of Pa) from the saturation temperature T_{sat}, which occurs at the physical interface between the gas and liquid phases (see Figure 3):

$$P_g(T_{sat}) = \frac{101356}{760} \cdot 10^{A - B/T_{sat}} \tag{6a}$$

This expression comes from the Fluorinert™ manual published by 3M.[15] A and B are FC-specific coefficients, as shown in Table I.

For liquid-only conditions in the cavity, the pressure associated with the liquid can be determined from Equations (3) and (5):

$$P_l(T_{sat}) = P_a + E \cdot \frac{2}{.0151 \cdot (1 - \boldsymbol{m}^2)} \cdot \frac{z_0}{a} \cdot \left(\frac{h}{a}\right)^3 \cdot \boldsymbol{h} \cdot \ln\left(\frac{C''-T_f}{C'' - \frac{T_{sat} + T_a}{2}}\right) \tag{6b}$$

Since the cavity is isobaric, the membrane deflection will be given by the maximum pressure in the cavity, whether determined from the gas or liquid phase. As shown below, the liquid phase can in fact become negative, leading to cavitation of a gas bubble in the cavity, in order to maintain positive absolute pressure in the cavity.

4.4 Solution

The solution of the steady-state behavior of the system then stems from solving:

$$z_g(T_{sat}) = z_l(T_{sat}) \cdot \frac{\boldsymbol{r_l}}{\boldsymbol{r_g}} \frac{T_r - T_{sat}}{T_{sat} - T_a} \tag{1b}$$

$$z_l(T_{sat}) = \boldsymbol{h}z_0 + \boldsymbol{dz_l}(T_{sat}) \tag{2b}$$

$$\boldsymbol{dz_l}(T_{sat}) = \boldsymbol{h}z_0 \ln\left(\frac{C''-T_f}{C'' - \frac{T_{sat} + T_a}{2}}\right) \tag{4b}$$

$$z_g(T_{sat}) = (1 - \boldsymbol{h})z_0 + \boldsymbol{dz_g}(T_{sat}) \tag{2a}$$

$$\Delta z(T_{sat}) = \boldsymbol{dz_l}(T_{sat}) + \boldsymbol{dz_g}(T_{sat}) = 0.0151 \cdot (1 - \boldsymbol{m}^2) \cdot a \cdot \left(\frac{a}{h}\right)^3 \cdot \frac{\max[P_l(T_{sat}), P_g(T_{sat})] - P_a}{E} \tag{5}$$

These expressions can be re-arranged to form the dimensionless, transcendental equation:

$$\boldsymbol{h}\left\{1 + \ln\left(\frac{C''-T_f}{C'' - \frac{T_{sat} + T_a}{2}}\right)\right\}\left\{1 + \frac{\boldsymbol{r_l}}{\boldsymbol{r_g}} \cdot \frac{T_r - T_{sat}}{T_{sat} - T_a}\right\} =$$
$$1 + 0.0151 \cdot (1 - \boldsymbol{m}^2) \cdot \frac{a}{z_0} \cdot \left(\frac{a}{h}\right)^3 \cdot \frac{\max[P_l(T_{sat}), P_g(T_{sat})] - P_a}{E} \tag{6}$$

Presuming an initial fill state which is in the sub-cooled liquid regime ($\boldsymbol{h}$=1), there are three regions of behavior for the system:
- Region I: Cavitation region. Mixed gas-liquid phase. $T_r > T_{sat} > T_a$.
- Region II: Liquid-only region. $T_r = T_{sat}$.
- Region III: Evaporation (boiling) region. Mixed gas-liquid phase. $T_r > T_{sat} > T_a$.

In Regions I and III, Equation (6) is solved to obtain T_{sat}. The stroke is then obtained from Equation (5), where the maximum pressure is given by P_g. In Region II, it is unnecessary to find the saturation temperature, and the relationship between stroke and resistor temperature is simply given by:

$$\Delta z(T_r) = 2\boldsymbol{h}z_0 \ln\left(\frac{C''-T_f}{C'' - \frac{T_r + T_a}{2}}\right) \tag{7}$$

Note that Equation (7) has no ambient pressure dependence, since the liquid in Region II fills the entire cavity, and the liquid is taken to be incompressible. Said another way, the internal cavity pressure will increase to whatever value is required to deliver a given stroke, despite changes in ambient pressure.

Note, too, that the stroke is affected only by the cavity depth, thermopneumatic fluid material properties, fill temperature, ambient temperature, and resistor temperature. That is, the membrane does *not* affect the stroke when the cavity is hydraulically locked.

5.0 RESULTS

In the following results, the ratio of thermal resistivities for the Fluorinert™, between liquid and gas phases, is not known. A ratio of 100 (gas phase being 100 times less thermally conductive than the liquid phase) is assumed.

Figure 5 shows the pressure versus resistor temperature results for a typical microvalve used in low-flow mass flow controllers.[9] FC-43 with T_f=38 ºC, h=1, z_0=100 µm, T_a=298 K, and P_a=101356 Pa are the relevant parameters. The crossover points between Regions I, II, and III are evident.

Figures 6 and 7 show the stroke versus resistor temperature for the same parameters as in Figure 5, except that ambient pressure, ambient temperature, and fill-seal temperature become additional variables. Several observations are noteworthy:
- Stroke in Region II is independent of ambient pressure.
- Stroke in Region I is dependent on ambient pressure; the higher the ambient pressure, the greater the negative stroke.
- Ambient temperature of 323 K for a fill temperature of 38 ºC creates a significant stroke, before power is even applied to the valve.
- Changes in ambient pressure do *not* shift the Region II behavior in temperature, even though the pull-in is changed.
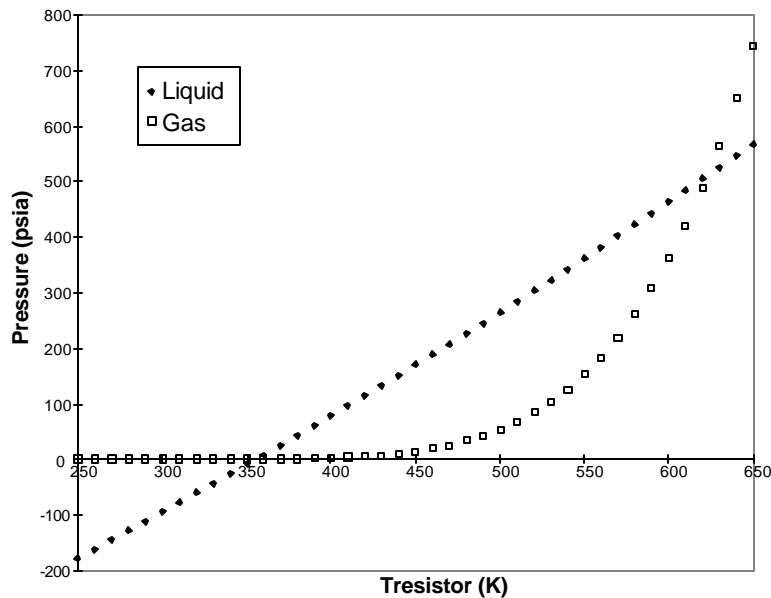

Figure 5*: Pressure versus resistor temperature for FC-43 with T_f=38 ºC, h=1, z_0=100 µm, T_a=298 K, and P_a=101356 Pa. The cavity pressure is the maximum of either the gas or liquid pressure. Note that the shrinking liquid, as the resistor temperature decreases, creates a negative pressure. Negative pressures are unphysical, but the cavitation creates a gas with a positive, though low, pressure, which determines the stroke in the FC cavity.*
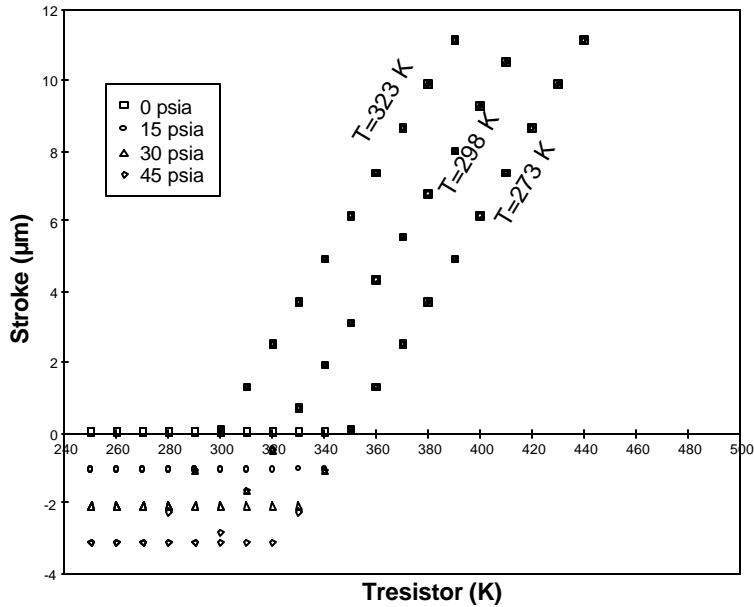
Figure 6: *Stroke versus resistor temperature for FC-43 with T_f=38 ºC, h=1, z_0=100 µm. Ambient temperature and ambient pressure are additional variables.*
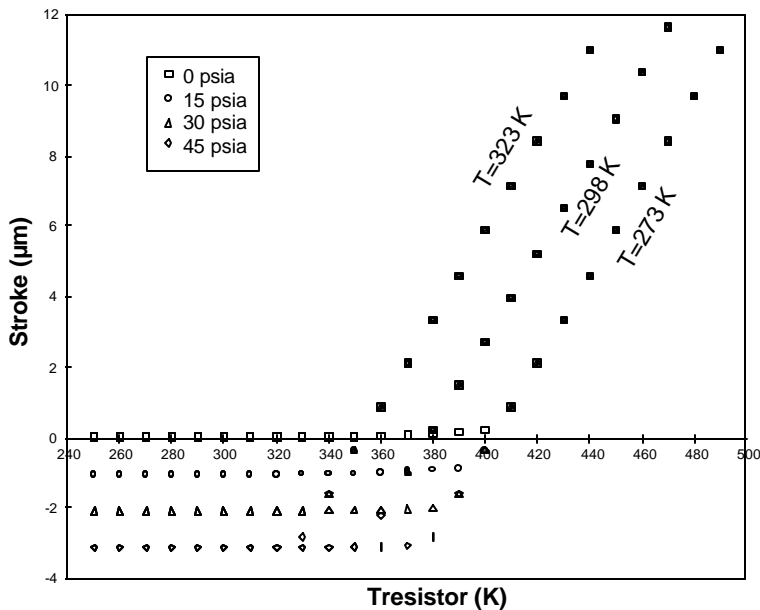
Figure 7: *Stroke versus resistor temperature for FC-43 with T_f=65 ºC, h=1, z_0=100 µm. Ambient temperature and ambient pressure are additional variables.*

6.0 APPLICATIONS TO MASS FLOW CONTROLLER VALVE DESIGN

6.1 Control of Flow (Stroke) at High Ambient Temperature

To achieve control over the stroke for high ambient temperature, two options are available: increase the fill temperature; or increase the initial gap between the membrane and the valve seat. Increasing the initial gap is not a desirable option, since this choice affects the flow model for the microvalve. Figures 6 and 7 show the effect of increasing the fill temperature. From a design perspective, the fill temperature should be chosen such that the stroke remains zero at the maximum ambient

temperature in the specification. Under this constraint, when the resistor temperature is equal to the ambient temperature (i.e., before power is applied to the valve):

$$\Delta z(T_r) = 2\boldsymbol{h}z_0 \ln\left(\frac{C''-T_f}{C''-\dfrac{T_r+T_a}{2}}\right) = 0$$

(8)

$$\Rightarrow T_f = T_a$$

6.2 Choice of Appropriate Thermopneumatic Fluid

Figure 8 shows a comparison between two Fluorinert™ fluids, using a fill temperature of 55 °C. As can be seen, though the slope of FC-43 is lower, it does not (because of its very low vapor pressure) suffer from 'stroke degradation' (the 'soft', gas-pressure-related portion of the stroke versus temperature curve for FC-84 around T=350 K) at ambient temperatures of 273 K. This behavior will maintain liquid-only mechanical expansion behavior in the microvalve. However, it comes at a penalty in power, since the higher boiling point Fluorinert™ fluids have lower coefficients of thermal expansion.
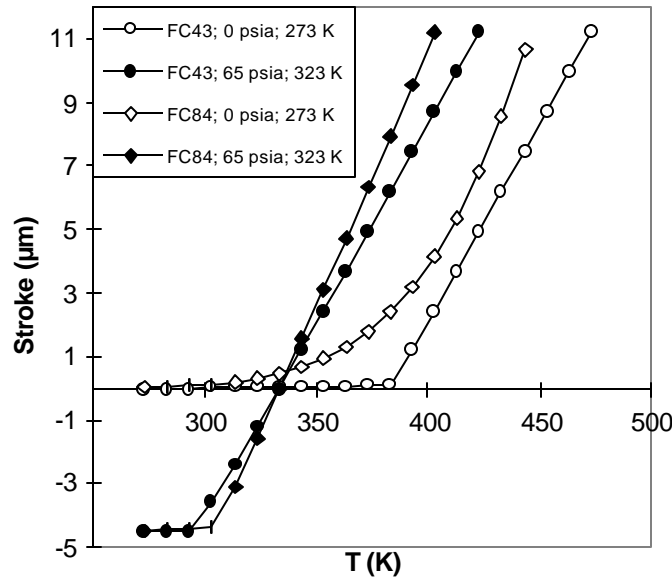

Figure 8: Stroke versus resistor temperature for two Fluorinert™ fluids. T_f=55 °C, $\boldsymbol{h}$=1, and z_0=100 µm.

6.3 Constraint: Threshold Temperature for Region III

For most stable control applications of thermopneumatically actuated microvalves, operation in Region III should be avoided. Setting Equations (6a) and (6b) equal, and finding T_{sat}, determines the threshold temperature for the transition to Region III behavior. This transcendental expression is difficult to solve (for instance, a Newton-Raphson method does not converge). Nonetheless, solutions are still available, even if only graphical. Figure 9 shows the results of comparing FC-43 and FC-84, for several values of ambient pressure and temperature. As suggested in Figure 5, it is clear there is a limit to the maximum resistor temperature, before the onset of evaporation/boiling. In fact, for FC-84, with P_a=0 psia, T_f=65 °C, and T_a=273 K, the cavity is always in the gas-liquid mixed phase state.

6.4 Constraint: Membrane Yield Strength

The stress in the membrane is determined by:[14]

$$\Delta z = 0.0491 \cdot (1 - \boldsymbol{m}^2) \cdot \boldsymbol{s} \cdot \frac{a^2}{Eh}$$

(8)

This expression is determined for a free membrane, with no load forces due to contact with, for instance, a valve seat. The limit for <111> silicon has been shown to be approximately 700 MPa.[16] Using this expression, for the membrane thicknesses and areas discussed above, this limit is reached for strokes exceeding 15 µm. The limit for <110> silicon fracture is 1.2 GPa, corresponding to a stroke of 25 µm. Mass flow controller microvalve data suggests over 50 µm of stroke can be achieved, with no significant fracture fallout.
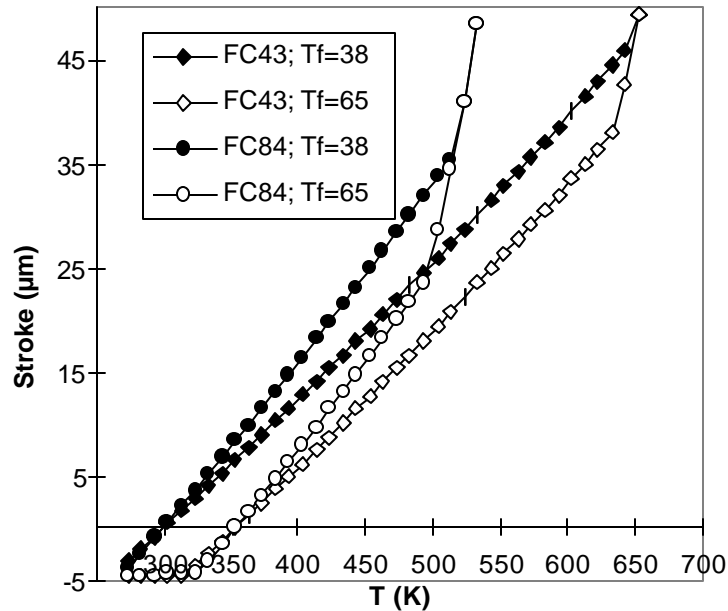

Figure 9: Stroke versus fill temperature and resistor temperature for FC-43 vs. FC-84. h=1 and z_0=100 µm.
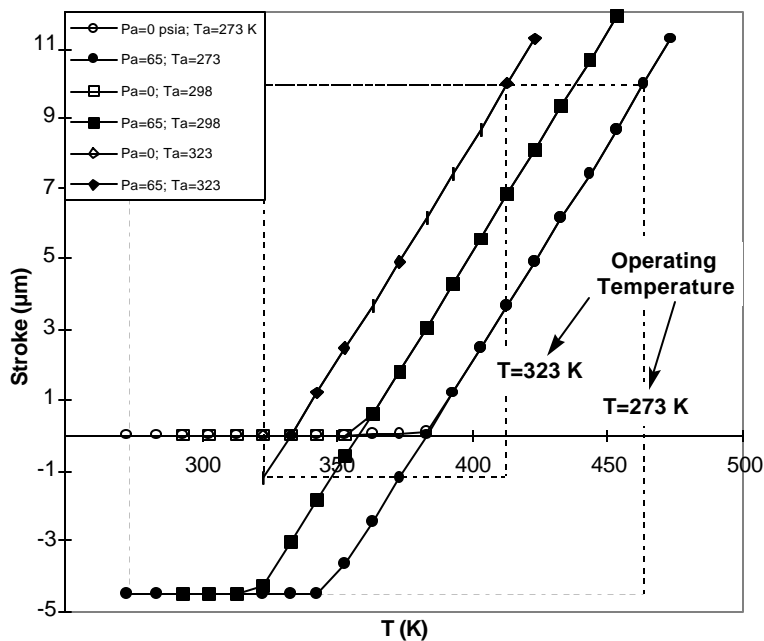

Figure 10: Overall operating range for a 10 µm stroke design. High and low ambient pressures are shown, as are low, mid, and high ambient temperatures. The effect of decreasing ambient temperature is to increase the power (temperature) required to reach 10 µm of actuation. The effect of increasing ambient pressure (pressure sensor pressure in the MFC design) is to increase the negative membrane stroke. Note that the maximum power is set by the ambient temperature,

independent of the ambient pressure. The design has full control of the stroke, from 0 to 10 µm, over the full range of ambient pressure and temperature.

7.0 MICROVALVE STROKE DESIGN FOR MASS FLOW CONTROL

Figure 10 shows the overall operating window for a 10 µm stroke design. This design is targeted for a 10 sccm maximum flow rate mass flow controller, with high resolution.[9] The specified operating temperature is 0 to 50 ℃. Control must be fully linear, with no transition to Region III. The fill temperature chosen to meet these specifications is 55 ℃, and the chosen Fluorinert™ fluid is FC-43. The fill factor h is equal to unity, while the cavity depth is 100 µm. Using these parameters, the relationship between stroke and resistor temperature is linear, and meets the design specifications, for the corners of a design space defined by low and high ambient temperature, and low and high ambient pressure.

8.0 CONCLUSIONS

We have demonstrated the development of a one-dimensional theory for the steady-state behavior of thermopneumatic fluids in a sealed cavity, including the effects of gas-liquid phase transitions, inhomogeneous thermal boundary conditions, ambient pressure fluctuations, and incomplete initial cavity filling. The impact of thermopneumatic fluids with varying thermodynamic properties has also been explored. We have applied this theory to the development of robust designs of silicon-based, thermopneumatically-actuated microvalves, used to control the flow and distribution of gases and liquids. Using the theory, a family of microvalves for use in high-resolution mass flow controllers has been generated successfully.

9.0 REFERENCES

1. M. Zdeblick, "A planar process for an electric-to-fluidic valve." Ph.D. dissertation, Stanford University, June, 1988.
2. P. W. Barth, "Silicon microvalves for gas flow control." In Proceedings, *Transducers '95 (1995 Int'l. Conf. Sol. State Sens. and Act.)*, pp. 276-279 (IEEE, Piscataway, NJ, 1995).
3. H. Jerman, "Electrically-activated, normally-closed diaphragm valves." In Proceedings, *Transducers '91 (1991 Int'l. Conf. Sol. State Sens. and Act.)*, pp. 1045-48 (IEEE, Piscataway, NJ, 1991).
4. J. D. Busch and A. D. Johnson, "Prototype micro-valve actuator." In Proceedings, *IEEE Micro Electro Mechanical Systems*, pp. 40-41 (IEEE, Piscataway, NJ, 1990).
5. T. Ohnstein, T. Fukiura, J. Ridley and U. Bonne, "Micromachined silicon microvalve." In Proceedings, *IEEE Micro Electro Mechanical Systems*, pp. 95-98 (IEEE, Piscataway, NJ, 1990).
6. C. Vieder, O. Öhman, and H. Elderstig, "A pneumatically actuated micro valve with a silicon rubber membrane for integration with fluid-handling systems." In Proceedings, *8th Int'l. Conf. Sol. State Sens. and Act.*, pp. 284-286 (1995).
7. D. Hopkins, "Electrochemical actuator, and method of making same." U.S. Patent 5,671,905 (1997).
8. M. J. Zdeblick and J. B. Angell, "A microminiature electric-to-fluidic valve." In Proceedings, *Transducers '87 (1987 Int'l. Conf. Sol. State Sens. and Act.)*, pp. 827-830 (IEEE, Piscataway, NJ, 1987).
9. A. K. Henning, "Microfluidic MEMS for semiconductor processing." In *Proceedings, 2nd Annual International Conference on Innovative Systems in Silicon*, pp. 340-349 (IEEE Press, Piscataway, NJ, 1997). To appear in *IEEE Trans. Comp. Packaging and Manuf. Tech.*
10. A. K. Henning, J. Fitch, E. Falsken, D. Hopkins, L. Lilly, R. Faeth, and M. Zdeblick, "A thermopneumatically actuated microvalve for liquid expansion and proportional control." In Proceedings, *Transducers '97 (1997 Int'l. Conf. Sol. State Sens. and Act.)*, pp. 825-828 (IEEE, Piscataway, NJ, 1997).
11. S. Shoji, B. Van der Schoot, N. de Rooij, and M. Esashi, "Smallest dead volume microvalves for integrated chemical analyzing systems." In Proceedings, *Transducers '91 (1991 Int'l. Conf. Sol. State Sens. and Act.)*, pp. 1052-5 (IEEE Press, Piscataway, NJ, 1991).
12. X. Yang, C. Grosjean, Y. C. Tai, and C. M. Ho, "A MEMS thermopneumatic silicone membrane valve," In Proceedings, *IEEE Micro Electro Mechanical Systems Workshop,* pp. 114-118 (IEEE, Piscataway, NJ, 1997).
13. W. R. McGillis, V. P. Carey, J. S. Fitch, and W. R. Hamburgen, "Boiling behavior of aqueous mixtures at atmospheric and subatmospheric pressure." In Proceedings, *28th National Heat Transfer Conference*, pp. 139-148 (ASME, New York, 1992).
14. Mario di Giovanni, Flat and Corrugated Diaphragm Design Handbook. (Marcel Dekker, New York, 1982)
15. "Product Manual: "Fluorinert Electronic Liquids." (3M Industrial Chemical Products Division, 3M Corporation, St. Paul, MN,1990)

16. C. J. Wilson and P. A. Beck, "Fracture testing of bulk silicon microcantilever beams subjected to a side load." *J. Microelectromech. Syst.* **5**, pp. 142-150 (1996).